Journal of Alloys and Compounds 508 (2010) 338–341

Contents lists available at ScienceDirect

Journal of Alloys and Compounds

journal homepage: www.elsevier.com/locate/jallcom

$BaNiSn_3$-type ternary germanides $SrMGe_3$ (M = Ir; Pd and Pt)

H. Fujii [a,*], A. Sato [b]

[a] Superconducting Materials Center, National Institute for Materials Science, 1-2-1 Sengen, Tsukuba, Ibaraki 305-0047, Japan
[b] Materials Analysis Station, National Institute for Materials Science, 1-1 Namiki, Tsukuba, Ibaraki 305-0044, Japan

ARTICLE INFO

Article history:
Received 15 June 2010
Received in revised form 11 August 2010
Accepted 25 August 2010
Available online 9 September 2010

Keywords:
Intermetallics
Crystal structure
X-ray diffraction
Magnetic measurements

ABSTRACT

Ternary intermetallics $SrMGe_3$ (M = Rh, Ir, Ni, Pd and Pt) have been prepared by arc melting. The crystal structure of these intermetallics was determined by single-crystal X-ray diffraction for M = Ir, Pd and Pt. The structure of those three intermetallics is $BaAl_4$-derivative $BaNiSn_3$-type with the space group $I4mm$ (No. 107). The other two, Rh and Ni, are likely to take the same structure, speculated from the corresponding XRD patterns using the powder samples. Neither of them shows superconductivity down to 1.8 K.

1. Introduction

Among ternary intermetallic compounds, $ThCr_2Si_2$-type intermetallics have been extensively studied, especially for the interest of the superconducting and magnetic properties. The structure of $ThCr_2Si_2$ is the ordered ternary derivative of the binary $BaAl_4$-type structure [1]. Although superconductivity is observed for some compounds, the critical temperature (T_c) is generally very low, as reported for $LaPd_2Ge_2$ and $LaIr_2Ge_2$ with T_c's of 1.12 [2] and 1.5 K [3], respectively. Many works were carried out for the discovery of new intermetallic superconductors with higher T_c's. Finally, quaternary intermetallic superconductors AT_2B_2C with $ThCr_2Si_2$-derivative structure showing high T_c's were discovered [4–7]. Among these borocarbides, YPd_2B_2C shows the highest T_c of 23 K. Furthermore, recently new $ThCr_2Si_2$-type superconductors $(Ba,Sr)_{1-x}(K,Cs)_xFe_2As_2$ were discovered with T_c's up to 38 K [8,9]. Thus, this structure is one of the keys to search for new high-T_c intermetallic superconductors. Indeed, we have recently discovered $ThCr_2Si_2$-type ternary germanide $SrPd_2Ge_2$ shows superconductivity with a T_c of 3.0 K [10]. Other related germanides SrM_2Ge_2 (M = Ni and Ir) with the same $ThCr_2Si_2$-type structure do not show superconductivity down to 1.8 K [11].

Numerous intermetallics with this $ThCr_2Si_2$-type structure have been reported. The $ThCr_2Si_2$-type structure is one of the derivatives of the binary $BaAl_4$-type structure, as mentioned above. The intermetallics with other derivative structures such as $CaBe_2Ge_2$ and $BaNiSn_3$ have been much less reported. The structural difference among these three types in A–M–X ternary systems is as follows: XMX–XMX in $ThCr_2Si_2$, MXM–XMX in $CaBe_2Ge_2$, MXX–MXX in $BaNiSn_3$. In this paper we report new $BaNiSn_3$-type intermetallics $SrMGe_3$ (M = Ir, Pd and Pt). Neither of them shows superconductivity down to 1.8 K.

2. Experimental

Starting materials were Sr (sheet, 99% in purity), Rh (powder, 99.9%), Ir (powder, 99.9%), Ni (shot, 99.9%), Pd (sheet, 99.95%), Pt (sheet, 99.95%) and Ge (grain, 99.99%). The Rh and Ir powders were preliminary arc melted to form small grains. They were arc melted with a stoichiometric ratio of $SrMGe_3$ (M = Rh, Ir, Ni, Pd and Pt) under Ar gas atmosphere on a water-cooler copper hearth. The melting was repeated several times with the button turned over between each melt. First M and Ge were arc melted, and then the melted buttons were melted together with Sr in order to minimize the loss of Sr. The weight loss after the melting was within a few percent. The obtained buttons wrapped in a Ti foil were annealed in an evacuated silica tube at 1173 K for one week and quenched into a cold-water bath.

Phase identification was carried out for crushed samples by an X-ray diffraction (XRD) method with an X-ray diffractometer Rigaku RINT-TTR III with monochromatized Cu $K\alpha$ radiation. Single crystals for structural analyses picked up from the crushed samples were glued on the top of a glass fiber and mounted on the goniometer head. X-ray single crystal diffraction data were collected at room temperature 293(2) K using a Bruker SMART APEX CCD area-detector diffractometer with graphite monochromatized Mo $K\alpha$ radiation (λ = 0.071073 nm). The absorption correction and structural refinement were carried out using the programs SADABS and SHELXL97 [12–14].

Microstructural observation was carried out using a scanning electron microscope (SEM) JEOL JSM-6301F with an energy dispersive X-ray (EDX) spectrometer.

DC magnetization measurements were performed for polycrystalline bulk samples at temperatures above 1.8 K with a superconducting quantum interference device (SQUID) magnetometer Quantum Design MPMS XL. Each measurement was carried out for a few samples to check reproducibility.

* Corresponding author. Tel.: +81 0 29 859 2326; fax: +81 0 29 859 2301.
E-mail address: fujii.hiroki@nims.go.jp (H. Fujii).

0925-8388/$ – see front matter © 2010 Elsevier B.V. All rights reserved.
doi:10.1016/j.jallcom.2010.08.150

Table 1
Atomic coordinates and equivalent thermal parameters for $BaNiSn_3$-type $SrMGe_3$ (M = Ir, Pd and Pt).

Site	Atom	Wyckoff position	x	y	z	$U_{eq} \times 10^4$ (nm^2)
Sr	Sr	2*a*	0	0	0.0000(3)[1]	1.49(4)[1]
					0.0000(2)[2]	1.45(3)[2]
					0.0000(2)[3]	1.50(3)[3]
M	*M*	2*a*	0	0	0.6493(1)[1]	1.21(2)[1]
					0.6419(1)[2]	1.23(2)[2]
					0.6448(1)[3]	1.30(1)[3]
Ge1	Ge	4*b*	0	1/2	0.2537(2)[1]	1.52(4)[1]
					0.2532(1)[2]	1.34(2)[2]
					0.2570(1)[3]	1.41(3)[3]
Ge2	Ge	2*a*	0	0	0.4123(2)[1]	1.55(5)[1]
					0.3994(2)[2]	1.43(4)[2]
					0.4012(2)[3]	1.38(4)[3]

Superscripts 1, 2 and 3 indicate the parameters for M = Ir, Pd and Pt, respectively.

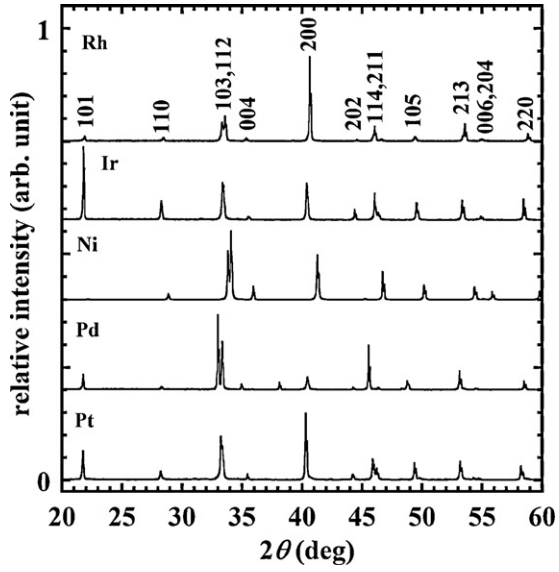

Fig. 1. XRD patterns of crushed polycrystalline samples of $SrMGe_3$ (M = Rh, Ir, Ni, Pd and Pt). Most of the XRD peaks are indexed on the basis of a tetragonal unit cell.

3. Results and discussion

Fig. 1 shows the XRD patterns of crushed powder sample $SrMGe_3$ (M = Rh, Ir, Ni, Pd and Pt). Most of the diffraction peaks in the XRD patterns are indexed on the basis of a tetragonal unit cell. The reflection condition of $h + k + l = 2n$. This indicates that the lattice is body centered with one of suggested space groups $I\bar{4}m2$, $I\bar{4}2m$, $I4mm$, $I422$ and $I4/mmm$. The lattice parameters of $SrIrGe_3$ are $a = 0.446$ and $c = 1.010$ nm. The $SrMGe_3$ with the other M's show the lattice parameters almost equal to those of $SrIrGe_3$. The color of $SrRhGe_3$ and $SrIrGe_3$ is slightly red, the same as $ThCr_2Si_2$-type $SrNi_2Ge_2$ and $SrPd_2Ge_2$, whereas the other intermetallics $SrNiGe_3$, $SrPdGe_3$ and $SrPtGe_3$ are metallic gray. Preliminary experiment revealed that arc melting of $SrMGe_3$ (M = Fe, Ru, Os and Co) did not form this tetragonal phase at all.

SEM–EDX analyses were performed on the polished cross-section of the buttons of $SrMGe_3$. The metallographic observation indicated that these samples were nearly single-phase, in agreement with the XRD patterns shown in Fig. 1. The composition of the main phase in these samples is Sr:M:Ge = 1:1:3, indicating that the phase with the tetragonal cell is indeed $SrMGe_3$.

Shiny crystals picked up from crushed samples of M = Ir, Pd and Pt were used for structural refinement. Preliminary investigations indicated that these crystals had almost the same lattice parameters as the polycrystalline $SrMGe_3$. The lattice parameters of $SrMGe_3$ are almost equal to those of $LaIrGe_3$ with $a = 0.4428(4)$ and $c = 1.0042(9)$ nm and $BaPtGe_3$ with $a = 0.45636(2)$ and $c = 1.023416(6)$ nm [15,16]. The structure of these intermetallics is $BaNiSn_3$-type with the space group $I4mm$ (No. 107). Therefore, the structural refinements were firstly carried out on the basis of the model of $BaNiSn_3$-type structure for $SrMGe_3$.

Table 1 lists the atomic coordinates and equivalent thermal parameters for $SrMGe_3$ (M = Ir, Pd and Pt). The crystal data and the results of structural refinements are listed in Table 2. The small R factors for these three intermetallics indicate that the structure of $SrMGe_3$ is $BaNiSn_3$-type. The difference of the number of refined parameters in Table 2 is associated with the extinction effect. The effect was ignorable for both $SrPdGe_3$ and $SrPtGe_3$ samples. Fig. 2 shows the crystal structure of $BaAl_4$, together with its derivative $BaNiSn_3$-type $SrMGe_3$ and $ThCr_2Si_2$. For the other two, $SrRhGe_3$

Table 2
Crystal data and results of the structural refinements for $BaNiSn_3$-type $SrMGe_3$ (M = Ir, Pd and Pt).

Compound	$SrIrGe_3$	$SrPdGe_3$	$SrPtGe_3$
Space group		$I4mm$ (No. 107)	
Formula units/cell		$Z = 2$	
Calculated density (gcm^{-3})	8.213	6.685	8.178
Crystal size (μm^3)	$40 \times 40 \times 100$	$60 \times 100 \times 100$	$60 \times 80 \times 160$
Absorption coefficient (mm^{-1})	68.031	38.81	69.020
R_{int}	0.0288	0.0315	0.0518
$2\theta_{max}$	80.48	80.42	80.84
Number of measured reflections	2262	2271	2140
Number of unique reflections	374	415	417
Number of reflections with $I > 2\sigma(I)$	374	413	415
$h\,k\,l$ range	$-8 \le h \le 8$, $-7 \le k \le 8$, $-12 \le l \le 18$	$-8 \le h \le 7$, $-8 \le k \le 8$, $-18 \le l \le 17$	$-7 \le h \le 8$, $-7 \le k \le 7$, $-18 \le l \le 18$
Number of refined parameters	15	14	
Final residual $R[F^2 > 2\sigma(F^2)]$	0.0401	0.0431	0.0342
Weighted R (F^2)	0.1106	0.1018	0.0825
Goodness of fit on F^2	1.101	1.119	1.104
$\Delta\rho_{max}/\Delta\rho_{min}$ (e/Å^3)	3.001/−4.508	2.434/−1.585	4.380/−2.319

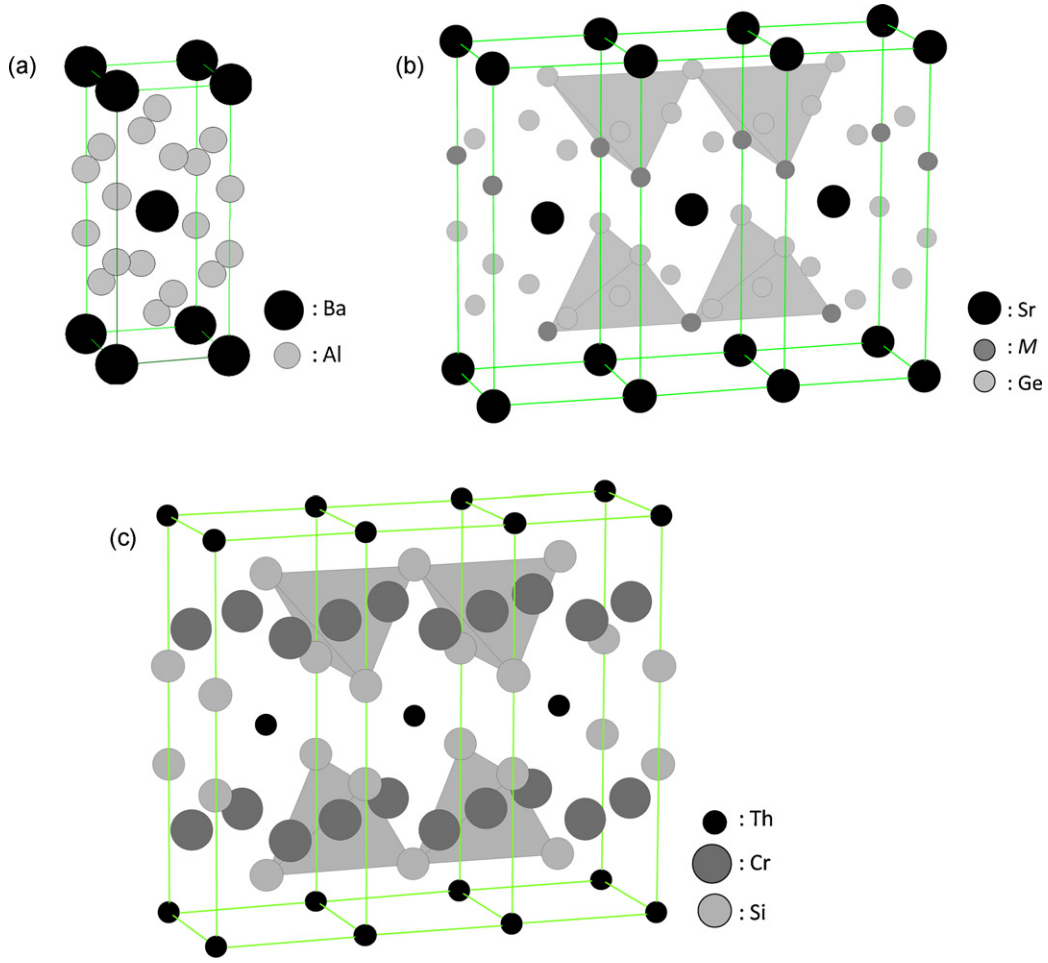

Fig. 2. Crystal structure of (a) $BaAl_4$, together with its derivative (b) $BaNiSn_3$-type SrMGe$_3$ (M = Ir, Pd and Pt) with Ge(2)M_2Ge(1)$_2$ tetrahedra and (c) $ThCr_2Si_2$ with $CrSi_4$ tetrahedra.

and $SrNiGe_3$, we could not pick up single crystalline samples. The lattice parameters of those two intermetallics suggest that they are likely to take the same $BaNiSn_3$-type structure and Rietveld structural refinements using the XRD patterns of those polycrystalline samples are under way.

Table 3 lists the lattice parameters, atomic radii r_i [17], interatomic distances d_{i-j} and their corresponding relative dilatations Δ_{i-j} in SrMGe$_3$ (M = Ir, Pd and Pt), together with $ThCr_2Si_2$-type SrM'_2Ge_2 (M' = Ir, Ni and Pd) for comparison [10,11]. Here Δ_{i-j} is defined as $\Delta_{i-j} = \left(d_{i-j} - \sum r_i\right) / \sum r_i$. The axial ratio c/a is almost the same for $BaNiSn_3$-type ternary germanides AMGe$_3$, ranging from 2.24 in $BaPtGe_3$ [16] to 2.30 in $SrPdGe_3$. Small atoms such as Y at the 2a site in AMGe$_3$ have not been reported so far and the decrease in size of the atom A at the 2a site in the AMGe$_3$ turns the structure to cubic $Yb_3Rh_4Sn_{13}$-type with similar composition [15].

On the other hand, in the $ThCr_2Si_2$-type AM_2Ge_2 the c/a ratio ranges from 2.29 in $LaPd_2Ge_2$ to 2.73 in YMn_2Ge_2 [18,19]. The decrease in size of the atom A at the 2a site in AM_2Ge_2 does not always decrease the c-axis parameter. This relatively large range of the c/a ratio in $ThCr_2Si_2$-type, compared with $BaNiSn_3$-type, is associated with the ability of accommodating various combinations of three atoms. Hence, a huge number of intermetallic compounds with this structure are observed. On the other hand, the small range of the c/a ratio in $BaNiSn_3$-type means a smaller number of intermetallics with this structure.

These $ThCr_2Si_2$- and $BaNiSn_3$-type structures have layers of M'Ge$_4$ and Ge(2)M_2Ge(1)$_2$ tetrahedra, respectively, as shown in Fig. 2. These layers are connected with Ge–Ge and M–Ge(1) bonds. The $\Delta_{M-Ge(1)}$ in SrMGe$_3$ is almost equal and small, suggesting strong interactions between the layers of the Ge(2)M_2Ge(1)$_2$ tetrahedra. On the other hand, the Δ_{Ge-Ge} in SrM'_2Ge_2 is scattered and large, suggesting weak interactions between the layers. Other $ThCr_2Si_2$-type ternary germanides also show such scattered Δ_{Ge-Ge}, ranging from −11.3 in YCu_2Ge_2 to +4.2 in $SrRu_2Ge_2$ [19,20]. Therefore, the difference of the interactions between the layers causes the difference of range in the c/a ratio and hence the number of intermetallics for these two structures.

Fig. 3 shows temperature-dependent DC magnetization curves measured in both zero-field cooling (ZFC) and field cooling (FC) modes for polycrystalline samples of SrMGe$_3$ (M = Ir, Pd and Pt). The $SrPdGe_3$ sample does not show diamagnetic signals down to 1.8 K, indicating that the sample is not superconducting. This is in contrast to $BaAl_4$-derivative $ThCr_2Si_2$-type $SrPd_2Ge_2$ with a T_c of 3.0 K [10].

On the other hand, the other two samples $SrIrGe_3$ and $SrPtGe_3$ show a diamagnetic signal at around 5 K with a broad transition. The magnitude of magnetic shielding signal after being corrected for demagnetization effects is below 1% of that estimated for perfect diamagnetism. Taking into account the volume fraction of $SrIrGe_3$ and $SrPtGe_3$ phases in the samples from XRD analyses shown in Fig. 1, we conclude that neither of $SrIrGe_3$ nor $SrPtGe_3$ is superconducting down to 1.8 K. In a binary system of Ir–Ge, IrGe shows superconductivity with a T_c of 4.7 K [21]. In ternary systems of A–Ir–Ge, some superconducting materials such as $La_3Ir_2Ge_2$ with a T_c of 4.7 K [22] have been reported so far. On the other hand, in a Pt–Ge system, PtGe shows superconductivity with a T_c of 0.4 K [23].

Table 3
Lattice parameters, atomic radii, interatomic distances and their corresponding relative dilatations in $BaNiSn_3$-type SrMGe$_3$ (M = Ir, Pd and Pt) and $ThCr_2Si_2$-type SrM'_2Ge$_2$ (M' = Ir, Ni and Pd) [10,11]. Here Δ_{i-j} is relative dilatations of the interatomic distances from atomic radii, defined as $\Delta_{i-j} = \left(d_{i-j} - \sum r_i\right) / \sum r_i$ where d_{i-j} and r_i denote interatomic distances of i–j and atomic radius of i, respectively. The radius of Ge used is 0.137 nm [17].

Compound	$SrIrGe_3$	$SrPdGe_3$	$SrPtGe_3$	$SrIr_2Ge_2$	$SrNi_2Ge_2$	$SrPd_2Ge_2$
Lattice parameters						
a (nm)	0.44653(1)	0.44623(2)	0.44778(2)	0.41916(2)	0.41801(1)	0.44088(2)
c (nm)	1.00909(5)	1.02737(7)	1.01366(9)	1.0674(1)	1.02409(6)	1.01270(8)
c/a	2.2598	2.3023	2.2637	2.5465	2.4499	2.2970
Cell volume (nm^3)	0.20120(1)	0.20457(2)	0.20325(2)	0.18753(2)	0.17894(1)	0.19684(2)
Atomic radius of M(M') (nm)	0.135	0.137	0.139	0.135	0.125	0.137
d_{Sr-M} (nm)	0.3499(1)	0.34758(8)	0.34901(8)			
	0.3539(3)	0.3679(2)	0.3600(2)			
$d_{Sr-Ge(1)}$ (nm)	0.3341(2)	0.3378(2)	0.3344(2)			
	0.3397(2)	0.3427(2)	0.3420(1)			
$d_{Sr-Ge(2)}$ (nm)	0.3279(1)	0.33202(8)	0.33209(8)			
$d_{M-Ge(1)}$ (nm)	0.24688(9)	0.25070(7)	0.25021(6)			
$\Delta_{M-Ge(1)}$ (%)	−9.2	−8.5	−9.3			
$d_{M-Ge(2)}$ (nm)	0.2391(3)	0.2491(2)	0.2470(2)			
$d_{Ge(1)-Ge(2)}$ (nm)				0.2766(3)	0.28332(7)	0.2626(1)
Δ_{Ge-Ge} (%)				+0.9	+3.4	−4.2

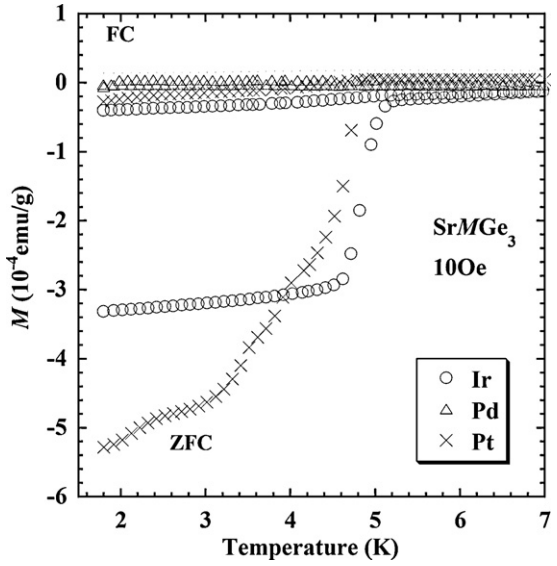

Fig. 3. Temperature-dependent DC magnetization curves for polycrystalline samples of SrMGe$_3$ (M = Ir, Pd and Pt). The data were recorded in both zero-field cooling (ZFC) and field cooling (FC) modes. The applied field was 10 Oe.

In the corresponding ternary system, $SrPt_4Ge_{12}$ shows superconductivity with a T_c of 5.4 K [24]. Therefore, the superconductivity observed in our samples is possibly due to the presence of such binary or ternary germanides.

$SrIrGe_3$ does not show superconductivity down to 1.8 K, as mentioned above. However, the color of the $SrIrGe_3$ sample is slightly red, the same as superconducting $SrPd_2Ge_2$. Therefore, $SrIrGe_3$ may show superconductivity below 1.8 K.

4. Conclusions

We have prepared ternary germanides SrMGe$_3$ (M = Rh, Ir, Ni, Pd and Pt) by arc melting. The germanides have a body-centered tetragonal unit cell with $BaNiSn_3$-type structure with the space group $I4mm$ (No. 107) for M = Ir, Pd and Pt, determined by single-crystal X-ray diffraction. The other two are also likely to take the same structure. DC magnetization measurements indicated that neither of them shows superconductivity down to 1.8 K.

References

[1] Z. Ban, M. Sikirica, Acta Crystallogr. 18 (1965) 594–599.
[2] G.W. Hull, J.H. Wernick, T.H. Geballe, J.V. Waszczak, J.E. Bernardini, Phys. Rev. B 24 (1981) 6715–6718.
[3] M. Francois, G. Venturini, J.F. Maréché, B. Malaman, B. Roques, J. Less-Common Met. 113 (1985) 231–237.
[4] R.J. Cava, H. Takagi, B. Batlogg, H.W. Zandbergen, J.J. Krajewski, W.F. Peck Jr., R.B. van Dover, R.J. Felder, T. Siegrist, K. Mizuhashi, J.O. Lee, H. Eisaki, S.A. Carter, S. Uchida, Nature 367 (1994) 146–148.
[5] R.J. Cava, H. Takagi, H.W. Zandbergen, J.J. Krajewski, W.F. Peck Jr., T. Siegrist, B. Batlogg, R.B. van Dover, R.J. Felder, K. Mizuhashi, J.O. Lee, H. Eisaki, S. Uchida, Nature 367 (1994) 252–253.
[6] R.J. Cava, B. Batlogg, T. Siegrist, J.J. Krajewski, W.F. Peck Jr., S. Carter, R.J. Felder, H. Takagi, R.B. van Dover, Phys. Rev. B 49 (1994) 12384–12387.
[7] H. Fujii, S. Ikeda, T. Kimura, S-i. Arisawa, K. Hirata, H. Kumakura, K. Kadowaki, K. Togano, Jpn. J. Appl. Phys. 33 (1994) L590–L593.
[8] M. Rotter, M. Tegel, D. Johrendt, Phys. Rev. Lett. 101 (2008) 107006(1)–1107006(4).
[9] K. Sasmal, B. Lv, B. Lorenz, A.M. Guloy, F. Chen, Y.-Y. Xue, C.-W. Chu, Phys. Rev. Lett. 101 (2008) 107007(1)–1107007(4).
[10] H. Fujii, A. Sato, Phys. Rev. B 79 (2009) 224522(1)–1224522(5).
[11] H. Fujii, A. Sato, J. Alloys Compd. 487 (2009) 198–201.
[12] G.M. Sheldrick, SADABS. Program for Empirical Absorption Correction of Area Detector Data, Univ. of Göttingen, 1996.
[13] Bruker, SMART, SAINT and SADABS, Bruker AXS Inc., Madison, WI, USA, 2001.
[14] G.M. Sheldrick, Acta Crystallogr. A64 (2008) 112–122.
[15] G. Venturini, M. Méot Meyer, B. Malaman, B. Roques, J. Less-common Met. 113 (1985) 197–204.
[16] R. Demchyna, Yu. Prots, W. Schnelle, U. Burkhardt, U. Schwarz, Z. Kristallogr. NCS 221 (2006) 109–111.
[17] E. Teatum, K. Gschneider, J. Waber, in: W.B. Pearson (Ed.), The Crystal Chemistry and Physics of Metals and Alloys, Wiley, New York, 1972, p. 151.
[18] G. Venturini, B. Malaman, J. Alloys Compd. 235 (1996) 201–209.
[19] G. Venturini, B. Malaman, B. Roques, J. Solid State Chem. 79 (1989) 136–145.
[20] J. González, R. Kessens, H.U. Schuster, Z. Anorg. Allg. Chem. 619 (1993) 13–16.
[21] B.T. Matthias, Phys. Rev. 92 (1953) 874–876.
[22] D.X. Li, S. Nimori, Y. Homma, Y. Shiokawa, A. Tobo, H. Onodera, Y. Haga, Y. Onuki, J. Appl. Phys. 97 (2005) 073903(1)–173903(6).
[23] B.T. Matthias, T.H. Geballe, V.B. Compton, Rev. Mod. Phys. 35 (1–22) (1963) 414.
[24] R. Gumeniuk, W. Schnelle, H. Rosner, M. Nicklas, A. Leithe-Jasper, Yu. Grin, Phys. Rev. Lett. 100 (2008) 017002(1)–117002(4).